A new interconnection technique for PV panel cells using cubic topology

Z. JAI ANDALOUSSI*, A. RAIHANI*, A. ELMAGRI* and O. BOUATTANE**

*Signal Distributed Systems and Artificial Intelligence Laboratory (SSDIA) of the Normal Superior School of Technical Education of Mohammedia ENSETM, BP 159 Mohammedia Principale, Morocco
**Hassan II University of Casablanca, Morocco, Laboratory Director
*Corresponding Author: jaiandaloussizakariae@gmail.com

ABSTRACT

This paper presents a new cells connection topology of the Photovoltaic panel. The idea is to interconnect the cells under a cubic topology. This configuration will be used to assess the impact of the shading scenarios on the performance of the panel and precisely the influence on the characteristics I-V and P-V. The Cubic and Series-Parallel configurations are studied using simulation models to compare their performances. Also, we studied their characteristic parameters as a function of the shading variations. This study concerns the open circuit voltage V_{oc}, the short-circuit current I_{sc}, and the maximum power P_{mp}, in order to find the best configuration that minimizes the effect of partial shade. The study of these performances is initiated for different shading scenarios: horizontal, vertical, diagonal, and random shading. The obtained results show that cubic topology can be considered as a solution for the problem of shading.

Keywords: Photovoltaic panel (PV); Series-Parallels configuration; Cubic configuration; Shading effect.

I. INTRODUCTION

The shading effect is a frequent phenomenon for photovoltaic panels; it reduces significantly the energy performance of PV systems (B. Patnaik et al., 2011). The losses due to the partial shading are not proportional to the shaded area but depend on the configuration of the cell's interconnection. The output power can be improved by distributing the shadow on different lines to maximize the output current of the PV panel (G. Velasco-Quesada et al., 2009). The severity of these effects can be reduced by amending the connections of the module of a solar panel. The use of solar energy has significantly grown in the last decades (Z. Mr Salameh et al., 1990). This is due to the increase of the energy demand. The depletion of conventional existing energy resources concerns more and more of the environmental problems and has increased the contribution of renewable energy sources to the total consumption. The solar energy is in the process of acquiring a lot of acclamation due to the decrease in the costs of photovoltaic cells and recent progress in technology for the photovoltaic power conversion. The generation of electricity by the PV panels also has several advantages; it is renewable, is eco-friendly, and is of low cost regarding the maintenance (B. A. Alsayid et al. 2013).

A PV panel is made up by several interconnected solar cells always in series or in parallel configurations, in order to increase the power output. The voltage of a photovoltaic module is usually chosen to be compatible with a storage voltage (S. Hamdi et al., 2014). Silicon Solar Cell has a voltage of 0.6V under the standard test conditions: Temperature 25°C and an irradiation of 1000W/m². If all the solar cells in a module have identical electrical characteristics, receiving

the same irradiation and temperature, then all cells operate exactly with the same current and voltage. In this case, the characteristics I-V and P-V of the module have the same form of the individual cells. The total current is simply the current of a cell multiplied by the number of cells in parallel, which is not the case for the real context.
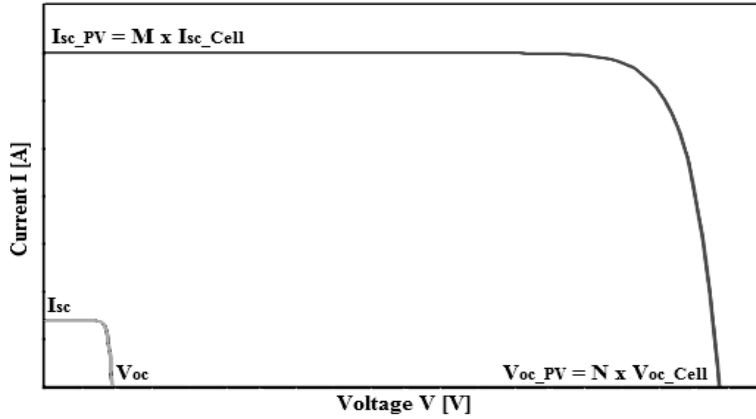
Figure 1. Feature I-V function of cells in series or in parallel.

$$V_{oc\_pv} = N \times V_{oc\_cell} \tag{1}$$

$$I_{sc\_pv} = M \times I_{sc\_cell} \tag{2}$$

With V_{oc} : Open circuit voltage [V],

I_{sc} : Short-circuit current of a cell [A],

N : Number of cells in series,

M : Number of cells in parallel.

In PV systems, it is practically impossible to avoid the shading problem; it may result from several forms such as the clouds, the trees, or the dust (Mr. Abdulazeez et al., 2005). Losses due to these anomalies are estimated at the loss of energy, thus reducing the rate of electricity production. The effects of this problem are identified by the presence of several peaks in the P-V characteristic function (K. Kurobe and al, 2005) (A. Ortiz-Conde et al, 2006). Clearly, the production of the cells is correlated with the incident light. It presents a serious problem in the photovoltaic cells, because the output of the whole PV panel in the worst conditions is determined by the cell with the lowest output. This can lead to local power dissipation and the cells heating, hence causing irreversible damage to the panel.

To solve this problem many configurations for PV cells connections were presented, such as the structure of Series-Parallel (SP) and Total Cross Tied (TCT) (Weidong Xiao et al, 2009) (Z. Shams El-Dein et al., 2013). Some studies proved that electrical reconfiguration techniques based on the Su-Du-Ko puzzle (N. D. Kaushika et al, 2007) or the Magic Square (MS) (V. Quaschning et al., 1990) were presented to disperse the shading effect from the surface of the PV panel. All these methods remain a two-dimensional configuration. In this paper, we propose a new technique to interconnect solar cells, based on the multidimensional topology and particularly the cubic one. This topology is studied and assessed for different shading scenarios.

The paper is organized as follows: Section II deals with an overview of the solar cells model, the standard Serie-Parallel configuration, and the proposed cubic circuit topology. In section III we present the materials and simulation results for different shading examples and IV gives some concluding remarks.

II. PHOTOVOLTAIC STRUCTURE

II.1. PV cell model

A PV panel consists of a number of PV cells in series, while the photovoltaic cell is modeled as a current generator parallel with one or two junctions. In this study, we choose the cell model with double exponential (E. Diaz-Dorado et al, 2010). Figure 2 shows the double-exponential model of a PV cell. This model includes

- A photo-current generated by the light in the cell. This photonic current I_{ph} is referred to as the quantity of light on the surface of the cell.

- Two diodes, representing the P-N junctions. Thus, junctions induce a potential barrier, which absorbs a current $I_D = I_{D1} + I_{D2}$.

- A parallel conductance $G_p = 1/R_p$, which represents the losses on the cells connections devices,

- A series resistance R_s which represents the Ohmic losses in the cell.

- The current I, which is the one that is really provided by the solar cell to a load under voltage V.
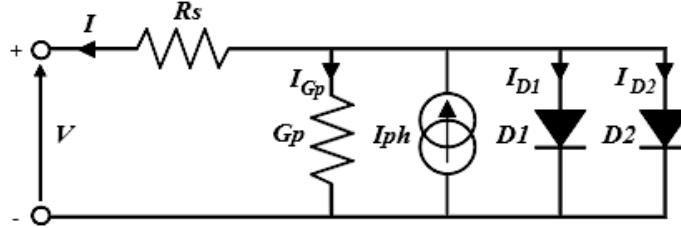
Figure 2. *Equivalent circuit PV cell.*

In Figure 2, the current I generated by the cell is the algebraic sum of four currents:

$$I = I_{ph} - I_{D1} - I_{D2} - I_{Gp} \tag{3}$$

The equation of the current in the diode is expressed by the Shockley relationship. Developing the relation (3), the expression of the PV cell current model is

$$I = I_{ph} - I_{01} \cdot \left[\exp\left(\frac{V_{cell} + R_s.I_{cell}}{n_1.v_{th}} \right) - 1 \right]$$
$$- I_{02} \cdot \left[\exp\left(\frac{V_{cell} + R_s.I_{cell}}{n_2.v_{th}} \right) - 1 \right] - G_p.(V + R_s.I_{cell}) \tag{4}$$

where I_{ph} : The photonic current is described by the equation:

$$I_{ph} = \left(\frac{G}{G_{ref}} \right) \times \left[I_{sc\_ref} + \mu_{cc}.(T - T_{ref}) \right] \tag{5}$$

with G, G_{ref} : real and reference irradiation [W/m²],

T, T_{ref} : ambient and reference temperature on the effective cell [K],

μ_{cc} : Temperature coefficient of the short-circuit current [A/K].

I_{01}, I_{02} : Reverse saturation current of the diodes 1 and 2,

$$I_{0i} = I_{0i}(T_i) \times \left(\frac{T}{T_{ref}}\right) \times \exp\left(\frac{-q.E_g}{n_i.k.\left(\frac{1}{T} - \frac{1}{T_{ref}}\right)}\right) \qquad (6)$$

E_g : Gap energy, (Eg=1.12eV for Silicon, Eg=0.66eV for Germanium),

n_1, n_2 : Quality Factor of the diodes 1 and 2,

v_{th} : Thermal voltage , $v_{th} = k.T/q$

k : Boltzmann constant (k=1.381.10^{-23} J/K),

q : Elementary charge of the electron (q=1.6.10^{-19} C).

Table 1 presents an example of an electrical settings photovoltaic cell, at 25°C, 1,5 Air mass (A.M), 1000 W/m2. The cell is made of 6 units of Figure 2, connected in series.

Table 1. The important settings of a PV Cell.

Solar Cell Parameters		
Parameter	**Label**	**Value**
Open circuit voltage	V_{oc}	4,067 V
Short circuit current	I_{sc}	1,75 A
Reverse saturation current of diode 1	I_{01}	2.34 10^{-8} A
Reverse saturation current of diode 2	I_{02}	7.02 10^{-5} A
Ideality factor of diode 1	n_1	1.27
Ideality factor of diode 2	n_2	1.54
Series resistance	R_s	0.05 Ω
Parallel resistance	R_p	10.72 Ω

II.2. Serie-Parallel Cell Arrangement

The cells of PV panel can be connected in many different ways. The well-known branches are the series and parallel ones. PV cells are connected in series and parallel to form a PV array in order to match the power requirements in terms of voltage and current. Cells connected in series are linked along a single path, so that the same current flow through them. Cells connected in parallel are linked, to show the same voltage. The total power in such an array is lower than the sum of the individual rated power of each cell (Abdulazeez et al, 2011). The main reason for that is the shading effect. In a series connected solar photovoltaic module, performances are severely affected if the cells are not equally illuminated. All the cells in a series array are forced to carry the same current even though a few cells under shade produce less photonic current. Shaded cells may get reverse biased, acting as loads, absorbing power from fully illuminated cells. If the system is not appropriately protected, a hot-spot problem can arise. In several cases, the system can be irreversibly damaged. In this article, we choose to study PV generator adapting this configuration, which is Serie-Parallel arrangement (SP).

The PV panel is composed of 12 cells arranged as three rows and four columns as in figure 3.
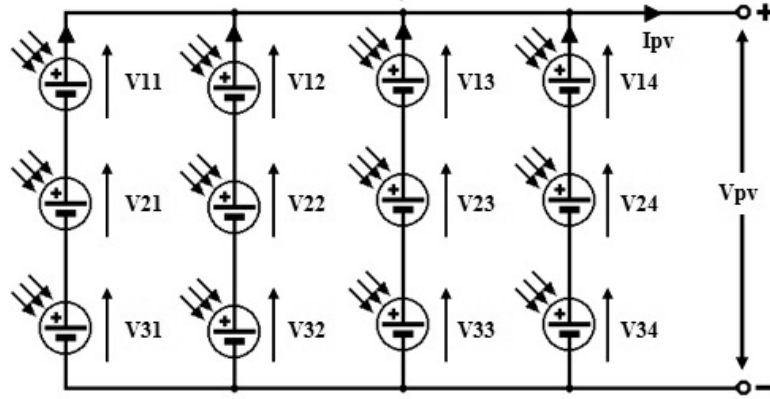
Figure 3. *PV panel using Series-Parallel (SP) Configuration.*

The generated current by a module for an irradiation *G* is given by

$$I_{pv} = \min(I_{11}, I_{21}, I_{31}) + \min(I_{12}, I_{22}, I_{32}) + \min(I_{13}, I_{23}, I_{33}) + \min(I_{14}, I_{24}, I_{34}) \tag{7}$$

with I_{ij} being the current generated by a cell located in the ith row and j^{th} column in the standard conditions (G_{ref} =1000 W/m² and *T*=25°C), since the expression of the photon current described in (5) becomes

$$I_{ph,ij} = \left(\frac{G_{ij}}{G_{ref}} \right) \times \left[I_{sc\_ref} + \mu_{cc}.(T - T_{ref}) \right] \tag{8}$$

with: G_{ij} being the irradiation received by the cell, which is in the *i*-row and the *j*-column. In our case, we have *i* = (1,2,3) and *j* = (1,2,3,4). This expression shows that the current of the PV panel is directly proportional to the solar irradiation of the panel.

The voltage at the terminals of the panel is given by the sum of the voltages along a column:

$$\begin{cases} V_{pv} = \max(V_{sj}) \\ V_{sj} = V_{1j} + V_{2j} + V_{3j} = \sum_{i=1}^{3} V_{ij} \end{cases} \tag{9}$$

In the Series-parallel (SP) connection, all the rows in series are disadvantaged, since any mismatch in I-V characteristics causes a reduction of the power and creates the hot spots.

II.3. PV Cubic topology:

Most structures almost used are flat. They are represented in the bidimensional configuration. The proposed structure in this paper is the cubic topology to interconnect the cells of the PV panel. The cubic topology is the three-dimensional representation of electrically equal and stackable square faces. It figures among the most remarkable configurations of three-dimensional space. It has 6 faces, 12 edges, and 8 vertices. The 3D PV generator is constituted by putting the cells in the cube edges.
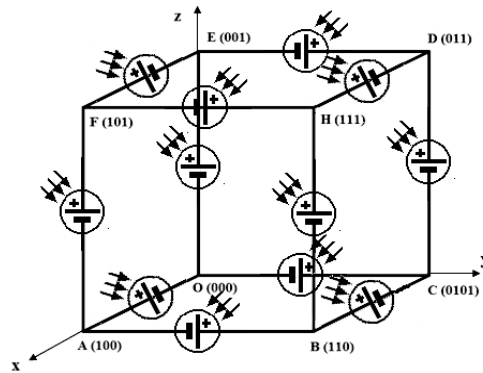
Figure 4. 3D Representation of the Cubic topology for the PV panel.

It is necessary to fix the cells polarization. The reason why a technique is based on the coding of the 3D axes is presented in Figure 4. The coding rule is based on the "Gray-code" to identify the neighboring nodes for each vertex. After defining the new 3D panel structure, it can be seen that the cubic configuration ensures the continuity of the current by multiple paths. This aspect can be considered as a benefit for the PV panel and especially can be used to reduce the losses caused by the shading effect.
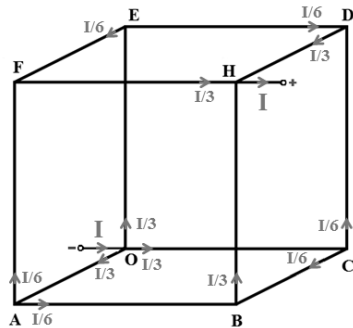
Figure 5. Distribution of the current in the cubic topology.

Figure 5 shows the distribution of the current in the cubic structure. In the *O* vertex, the current is divided into three identical quantities. On the other hand, we sum up the three quantities in the vertex *H*.
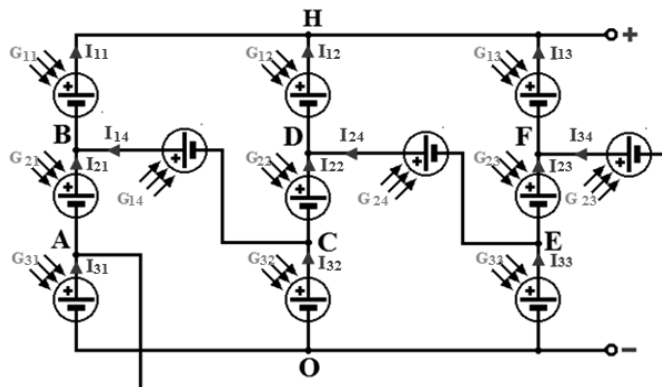
Figure 6. Distribution of the current in the flat cubic topology.

According to Figure 6, it can be seen that the current can follow six different paths between the two vertices O and H of the cube. The expression of the current delivered by the proposed 3D photovoltaic panel is

$$I_{pv} = I_{11} + I_{12} + I_{13} \tag{10}$$

By applying the node law to the electrical scheme of the figure 6. We can express the current in each node:

$$\begin{cases} \text{Node A}: I_{31} = I_{21} + I_{34} \\ \text{Node B}: I_{11} = I_{21} + I_{14} = I_{21} + I_{32} - I_{22} \\ \text{Node C}: I_{32} = I_{22} + I_{14} \\ \text{Node D}: I_{12} = I_{22} + I_{24} = I_{22} + I_{33} - I_{23} \\ \text{Node E}: I_{33} = I_{32} + I_{24} \\ \text{Node F}: I_{13} = I_{23} + I_{34} = I_{23} + I_{31} - I_{21} \end{cases} \tag{11}$$

In the case of balanced state, when the cells have the same characteristics and the same standard conditions (G=1000 W/m² and T=25°C), there will be

$$I_{11} = I_{12} = I_{13} = I_{Cell} \tag{12}$$

Therefore, the equation (12) will become

$$I_{pv} = 3 \times I_{Cell} \tag{13}$$

But there will be a change in nodes expressions; if all the panel are under the same irradiation, we will have

$$\begin{cases} \text{Node B}: I_{11} = \frac{I_{21} + I_{14}}{2} \\ \text{Node D}: I_{12} = \frac{I_{22} + I_{24}}{2} \\ \text{Node F}: I_{13} = \frac{I_{23} + I_{34}}{2} \end{cases} \tag{14}$$

By exploiting relation (10), it can be deduced that our configuration ensures the continuity of the current flow even if there is shading on any PV panel cell.

In the electrical circuit, we have 6 submeshes.

$$\begin{cases} V_{11} + V_{14} = V_{12} + V_{22} \\ V_{21} + V_{31} = V_{32} + V_{14} \\ V_{12} + V_{24} = V_{13} + V_{23} \\ V_{22} + V_{32} = V_{33} + V_{24} \\ V_{13} + V_{34} = V_{11} + V_{21} \\ V_{23} + V_{33} = V_{31} + V_{34} \end{cases} \tag{15}$$

The presence of 6 meshes in the diagram of Figure 6 leads to an internal stabilization at the level of the total PV panel voltage. Because there will always be a voltage drop compensation by the neighboring cells, which will confirm that the total voltage at the terminals of the panel is

$$V_{pv} = 3 \times V_{cell} \tag{16}$$

II.4. Material and experiment circuit

12 monocrystalline PV cells (156 mm x 156 mm x 0.2 mm) have the parameters mentioned in Table 1, mounted on two configurations. The first uses the SP array, and the second uses the proposed cubic topology. In order to study the effect of shading, the irradiation of the cells is controlled in a decreasing way. The decline in current cell production depends on the amount of shaded cell. Two types of shading experiments, namely, uniform and nonuniform, were performed. For uniform shading, the value of the irradiation is reduced to obtain a different shading percentage with a constant step. For nonuniform shading, different regions were selectively shaded using a random irradiation matrix. The I-V and P-V characteristics measurements were taken in each case. Each experiment was repeated at least three times to obtain coherent readings and the average values were reported. The output current and power were also determined for each experiment.

The expression of the irradiation matrix applied to the cell is

$$G = \begin{bmatrix} G_{11} & G_{12} & G_{13} & G_{14} \\ G_{21} & G_{22} & G_{23} & G_{24} \\ G_{31} & G_{32} & G_{33} & G_{34} \end{bmatrix} \qquad (17)$$

III.   RESULTS AND DISCUSSIONS

This section is devoted to the comparison by numerical simulations of the I-V and P-V characteristics for the two configurations SP and Cubic topologies. The irradiation levels of the cells depend on the environmental conditions, the state of the sky (clear or cloudy), and the location of the solar panel. During shading it has an influence on the photonics current I_{ph} of the cell, which is proportional to the solar irradiation G, that causes degradation for the total current issued from the PV panel. The performances of each configuration are achieved by plotting the PV characteristics for different types of shading patterns, namely, the horizontal axis, vertical, diagonal, and random (Dust effect) for the operation of the PV generator.

The rate of the shading effect from PV panel systems is studied by using formula (18). It calculates the average radiation distributed over the surface of the panel. It led us to a global study of different scenarios.

$$Shading\% = \left(G_{ref} - \frac{1}{N \times M} \sum_{i=1}^{N} \sum_{j=1}^{M} G_{ij} \right) \times 100\% \qquad (18)$$

III.1. Case of Horizontal shading

The cells of the PV generator are divided into four distinct groups. Group 1 represents the cells of the first column that receives an irradiation of 300 W/m², Group 2 receives 600 W/m², Group 3 receives 700 W/m², and Group 4 receives an irradiation of 900 W/m². This configuration presents the shading described in Figure 7. It notes that the shading disperses following the horizontal direction.
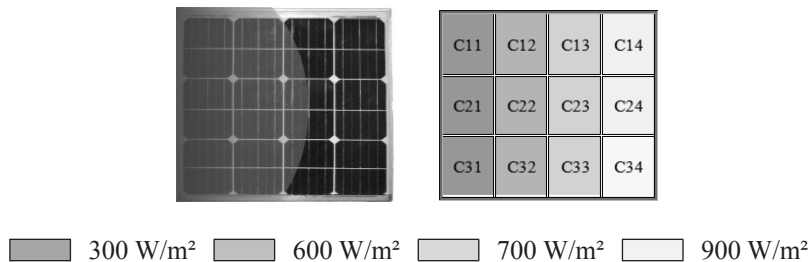
Figure 7. Horizontal distribution of the shading on the PV panel.

Figures 8 and 9 present the plotting of the I-V and P-V characteristics under the proposed horizontal shading configuration.
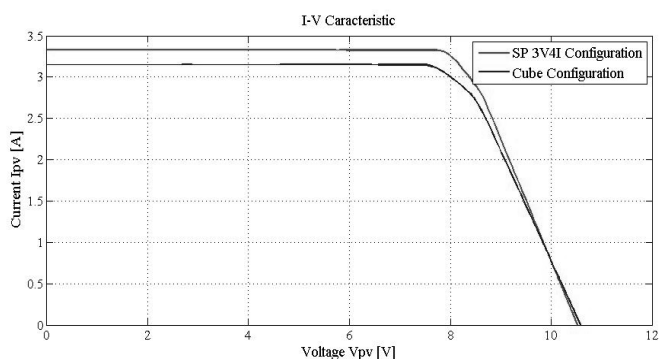
Figure 8. I-V characteristic under Horizontal shading.
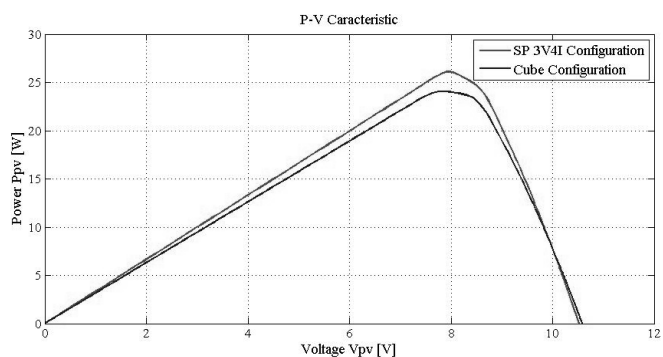
Figure 9. P-V characteristic under Horizontal shading.

Observing figures 8 and 9 the maximum power point values are 26.33 W and 24.67 W and the short circuit currents are 3.43A and 3.26A for the SP arrangement and the cubic configuration, respectively. For a shading of 35% a slight difference can be observed. The good performances of the cubic topology for this type of shading are shown on the table 2, which contains the values of the remarkable parameters in function of the rate of shading patterns for the two configurations.

Table 2. State "Horizontal Shading".

Shading %	Cubic Topology			SP Arrangement		
	I_{sc} [A]	V_{oc} [V]	P_{max}[W]	I_{sc} [A]	V_{oc} [V]	P_{max}[W]
0	5.25	12.2	40.72	5.25	12.2	50.68
5	4.9	11.97	38.43	5.075	11.97	39.76
15	4.725	11.6	36.12	4.725	11.53	35.99
25	4.2	11.15	32.57	4.375	11.08`	33.16
35	3.675	10.71	28.71	3.675	10.63	28.72
45	3.15	10.26	21.11	2.975	10.19	18.83
55	2.625	9.816	14.75	2.275	9.741	14.95
65	2.1	9.369	14.33	1.575	9.295	10.56
75	1.575	8.923	10.56	0.875	8.849	6.516
85	0.875	8.427	6.516	0.7	8.403	5.204

The comparison between the two arrangements is studied by plotting the maximum power characteristics for each panel as a function of the degree of shading.
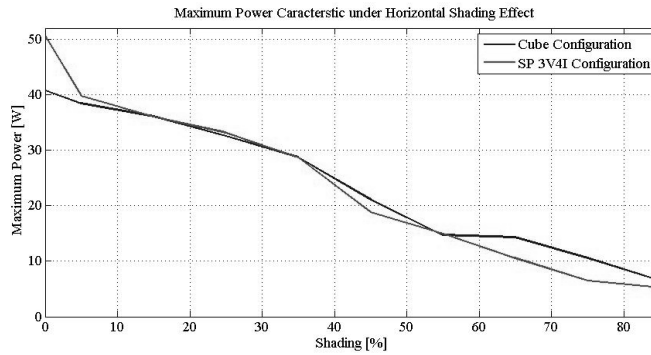
Figure 10. The maximum power versus the shading.

From a shading rate of 35%, the PV panel using the cubic configuration gives good results compared to SP arrangement.

III.2. Case of Vertical shading

The cells of the PV generator are divided into three distinct groups. Group 1 represents the cells of the first line, which receives an irradiation of 300 W/m², Group 2 receives (700 W/m²), and Group 3 receives an irradiation of 900 W/m². This example models the shading bias described in Figure 12. The shading disperses along the vertical axis.
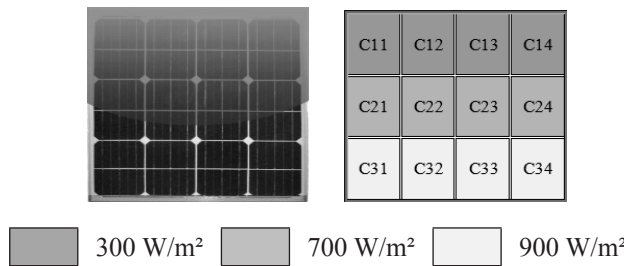
Figure 11. Vertical distribution of the shading on the PV panel.

The comparison between the two configurations is summarized on the I-V characteristics and P-V of figures 12 and 13.
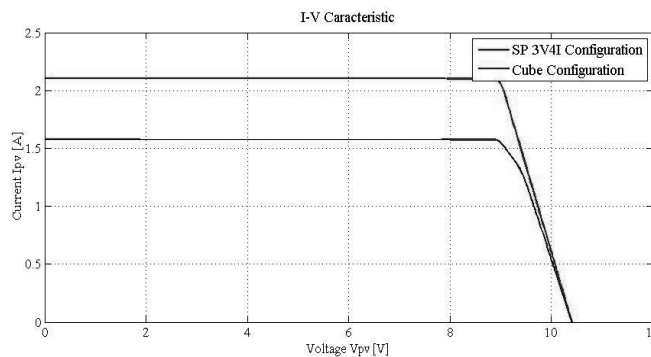
Figure 12. I-V characteristics under Vertical shading.
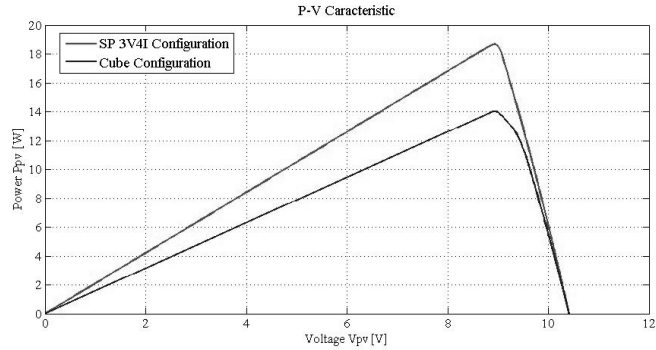
Figure 13. P-V characteristics under Vertical shading.

The horizontal shading presents a problem for the two configurations. This anomaly is reflected by the decreasing of the currents from each column of the PV panel, which decreases the total current. Table 3 contains the values of the short-circuit current, the voltage of open-circuit, and the maximum power depending on the degree of shading for the two configurations.

Table 3. State "Vertical Shading".

Shading %	Cubic Topology			SP Arrangement		
	I_{sc} [A]	V_{oc} [V]	P_{max}[W]	I_{sc} [A]	V_{oc} [V]	P_{max}[W]
0	5.25	12.2	40.72	7	12.2	50.68
5	4.725	12.02	39.74	6.3	12.02	44.35
15	4.2	11.75	35.67	5.6	11.75	37.39
25	3.675	11.3	30.98	4.9	11.3	34.61
35	3.15	10.86	26.38	4.2	10.86	31.93
45	2.625	9.13	24.99	3.5	9.13	26.06
55	2.1	9.964	22.21	2.8	9.964	16.68
65	1.575	9.518	13.2	2.1	9.518	14.68
75	1.05	9.072	8.673	1.4	9.072	9.248
85	0.525	8.626	4.255	0.7	8.626	5.213

According to the table 3, we note that the cubic configuration does not present a good result in this case of vertical shading.
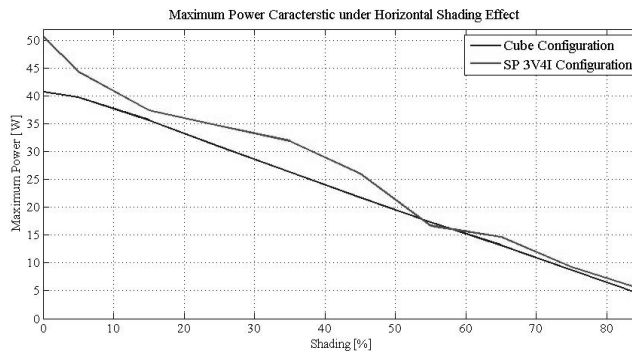
Figure 14. Maximum Power Characteristic under Vertical Shading Effect.

III.3. Case of Diagonal shading

In this case we deal with another interesting shading configuration. Figure 15 shows the solar panel under diagonal shading state at different levels.

According to the proposed distribution, we notify the I-V and P-V results as in figures 16-17.

C11	C12	C13	C14
C21	C22	C23	C24
C31	C32	C33	C34

◼ 300 W/m²   ◼ 500 W/m²   ◼ 700 W/m²   ◻ 900 W/m²
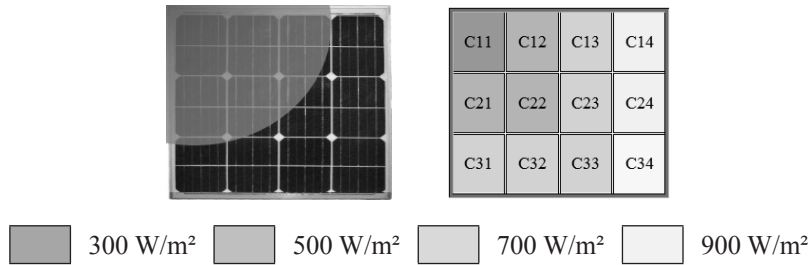
Figure 15. horizontal distribution of the shading on the PV panel.

Figures 16 and 17 present the plotting of the I-V and P-V characteristics under the proposed diagonal shading configuration.
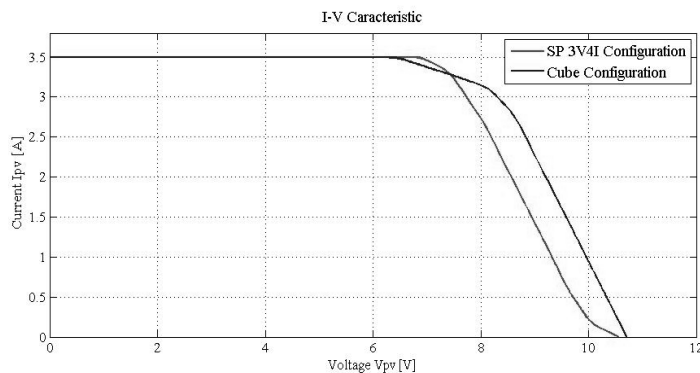
Figure 16. I-V characteristics under Diagonal shading.
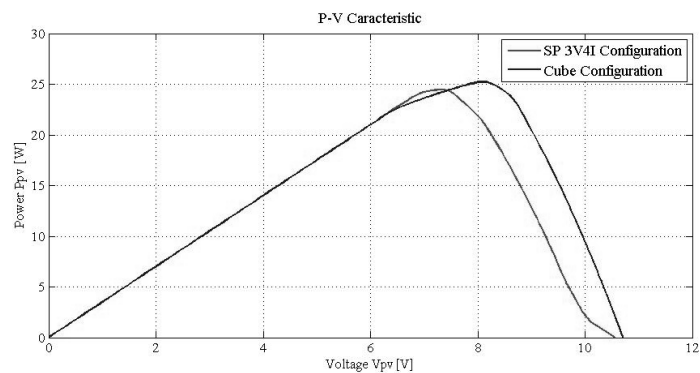
Figure 17. P-V characteristics under Diagonal shading.

The influence of the shading degree on the two panels is illustrated in Table 4, which contains the values of the remarkable parameters.

Table 4. State "Diagonal Shading".

Shading %	Cubic Topology			SP Arrangement		
	I_{sc} [A]	V_{oc} [V]	P_{max}[W]	I_{sc} [A]	V_{oc} [V]	P_{max}[W]
0	5.25	12.2	40.72	7	12.2	50.68
5	5.075	12.05	40.03	6.3	12.01	40.04
15	4.725	11.75	37.26	5.6	11.71	37.87
25	4.2	11.3	32.73	4.9	11.27	34.85
35	3.675	10.86	30.01	4.2	10.82	29.37
45	3.15	10.44	25.94	3.5	9.13	26.06
55	2.625	9.989	19.75	2.8	9.964	16.68
65	2.1	9.543	15.71	2.1	9.518	15.08
75	1.4	9.097	10.65	1.4	9.072	9.348
85	0.788	8.737	6.23	0.788	8.719	5.728
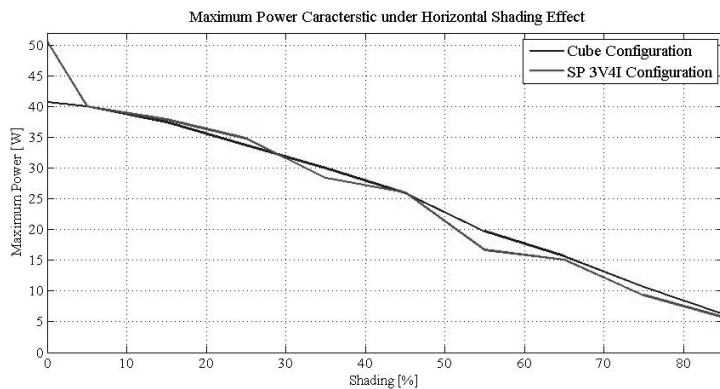
Figure 18. Maximum Power Characteristic under Diagonal Shading Effect.

As shown in the characteristic of the maximum power depending on the degree of shading, its reveals an important compensation effect presented by the cubic configuration compared to the SP configuration. This improvement comes from the three cells that complete the cube. Achieving the rate of 30% of the shade degree, the cubic configuration remains better than the SP one.

The comparison between the two configurations is summarized in Table 5 for the three previous shading effects.

Table 5. Remarkable parameters of the two configurations.

Case	Horizontal Shading		Vertical Shading		Diagonal Shading	
Panel Parameters	Cubic Topology	SP Arrang.	Cubic Topology	SP Arrang.	Cubic Topology	SP Arrang.
I_{pv}	2.4 x I_{cell}	2.5 x I_{cell}	0.9 x I_{cell}	1.2 x I_{cell}	2.7 x I_{cell}	2.5 x I_{cell}
V_{pv}	3 x V_{cell}	3 x V_{cell}	3 x V_{cell}	3 x V_{cell}	3 x V_{cell}	3 x V_{cell}
P_{mp}	7.2 x P_{cell}	7.5 x P_{cell}	2.7 x P_{cell}	3.6 x P_{cell}	8.1 x P_{cell}	7.5 x P_{cell}

III.4. Case of Random Shading 'Dust effect'

In this case, we study the two test arrangements under the random shading. This type of shading causes a random distribution of the solar radiation on the surface of the PV panel. It models the actual scenarios of the daily operation. The random shading can be viewed as the effect of dust. To model this case, we exploit the technique used in image processing; the dust is modeled by the effect of "pepper and salt (P&S)" noise, which is presented in Figure 19.
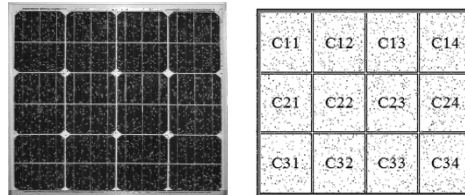
Figure 19. Random distribution of the shading on the PV panel.

In this case, we compare the characteristics of the two configurations on 3 random shadings.

To simulate the random shading, we use on the first test the following irradiation matrix:

$$G = \begin{bmatrix} G_{11} & G_{12} & G_{13} & G_{14} \\ G_{21} & G_{22} & G_{23} & G_{24} \\ G_{31} & G_{32} & G_{33} & G_{34} \end{bmatrix} = \begin{bmatrix} 397 & 883 & 576 & 737 \\ 289 & 199 & 492 & 703 \\ 778 & 681 & 915 & 970 \end{bmatrix} \tag{19}$$

The degree of shading for this test is about 36.5%, which means that we have an irradiation of 635 W/m² on the surface of the panel.
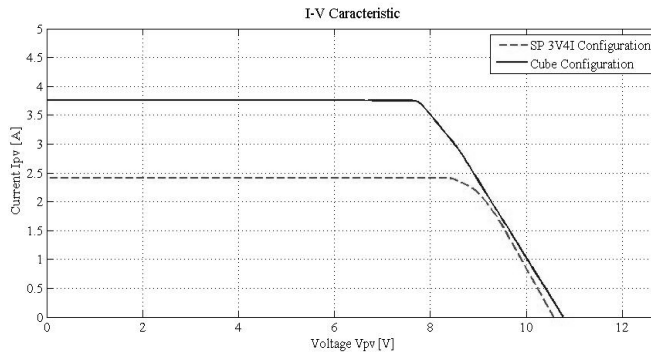
Figure 20. I-V characteristics under random shading.
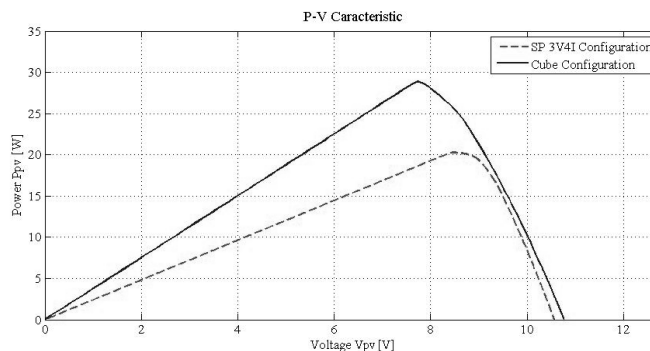
Figure 21. P-V characteristics under random shading.

Figures 20 and 21 show the simulated I-V and P-V characteristics for the two arrangements of solar PV panel under nonuniform irradiation conditions. It can be seen from the P-V characteristics that we find a maximum power peak of 20.25 W for the panel under the SP arrangement and a 28.88 W for the cubic configuration.

In the flowing second test, the irradiation matrix:

$$G = \begin{bmatrix} G_{11} & G_{12} & G_{13} & G_{14} \\ G_{21} & G_{22} & G_{23} & G_{24} \\ G_{31} & G_{32} & G_{33} & G_{34} \end{bmatrix} = \begin{bmatrix} 672 & 984 & 952 & 842 \\ 915 & 862 & 588 & 525 \\ 647 & 977 & 653 & 983 \end{bmatrix} \quad (20)$$

The mean irradiation on the surface of the panel is 799.8 W/m². We have a shading of 20.20%. The characteristics of I-V and P-V are shown in figures 22 and 23.
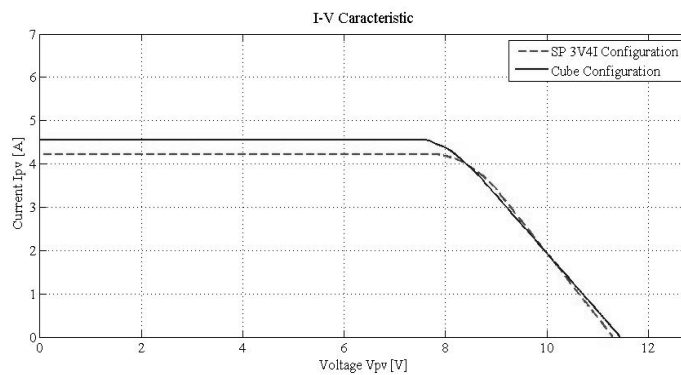
Figure 22. I-V characteristics under random shading.
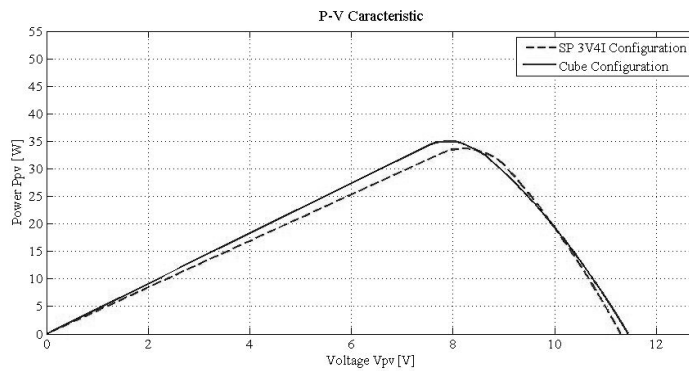
Figure 23. I-V and P-V characteristics under random shading.

In the third experiment we use the following irradiation matrix:

$$G = \begin{bmatrix} G_{11} & G_{12} & G_{13} & G_{14} \\ G_{21} & G_{22} & G_{23} & G_{24} \\ G_{31} & G_{32} & G_{33} & G_{34} \end{bmatrix} = \begin{bmatrix} 428 & 720 & 698 & 815 \\ 392 & 818 & 363 & 898 \\ 941 & 440 & 873 & 905 \end{bmatrix} \quad (21)$$

In this test the shading degree is about 30.91% and the average value of solar irradiation is 690,9 W/m² on the surface of the panel. Figures 24 and 25 present the plotting of the I-V and P-V characteristics under the proposed shading configuration.
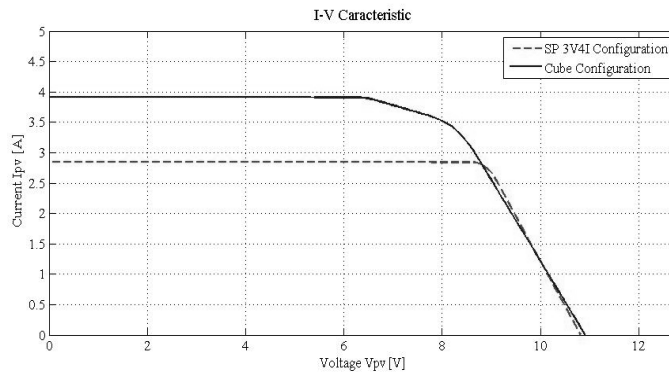
Figure 24. I-V characteristics under random shading.
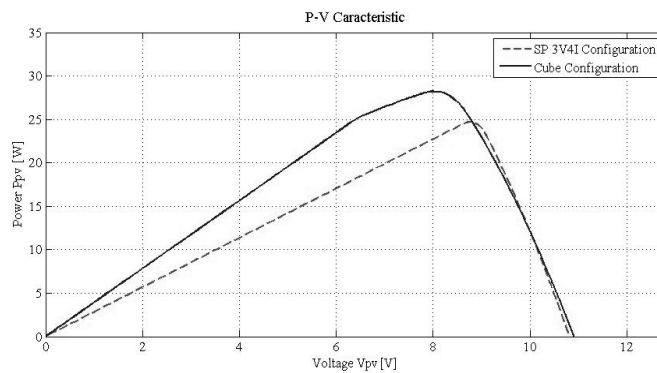
Figure 25. I-V and P-V characteristics under random shading.

To compare the two configurations, several attempts were made under random shading, while increasing the shading rate, and the maximum power for each PV panel was measured. The tests of the random shading effect on the two configurations are shown in Table 6.

Table 6. Maximum power point versus the shading effect for the two configurations.

Shading %	5.44	9.73	10.07	21.53	32.68	42.16	47.43	54.94	58.49
P_{max} Cubic Topology [W]	40.44	38.88	35.72	33.95	29.08	16.85	15.25	11.18	11.14
P_{max} SP Arrangement [W]	41.62	39.17	37.37	33.44	27.03	15.64	9.654	9.74	7.536

The table shows that when the shading rate increases the power produced by the cubic configuration is good compared to the SP configuration. This advantage comes from the fact that the C14, C24, and C34 cells prescribe the compensation. These cells ensure the continuity of the currant and the equilibrium of the potential difference in the photovoltaic panel. on the other hand, we see that the current produced by the panel under the cubic configuration came from 3 cells in parallel, unlike the parallel configuration whose current comes from the sum of 4 currents.

IV.   CONCLUSION

This article proposed the study of a new arrangement for PV cells using cubic topology. this arrangement is to improve the power output of the photovoltaic panel under shading effect conditions. The performances of the system

are studied through analysis and simulation for different types of shading patterns, in comparison with parallel seismic topology. According to the results, the cubic arrangement gives better results than the SP arrangement under diagonal and forward shading conditions, which is the case in the real world. The cubic arrangement allows the compensation of the losses and ensures the internal balance in voltage and current of the photovoltaic panel in case of default. the cubic topology has an inconvenient result, especially in the presence of shading on the cells (C14, C24, and C34), because they ensure the continuity of the electrical current.

REFERENCES

A. Ortiz-Conde, F. J. Garcia-Sanchez & Francisco J. Garcia-Sanchez "An Explicit Multi-exponential model as an alternative to traditional solar cell models with series and shunt resistances" ground. Energy Mater. Soil. Cells, Vol. 90, pp. 352-361, 2006.

B. Patnaik, P. Sharma, E. Trimurthulu, S. P. Duttagupta & V. Agarwal, "Reconfiguration strategy for optimization of solar photovoltaic array under non-uniform irradiation conditions", in *37th IEEE Photovoltaic Specialists Conference (PVSC)*, June 19-24, 2011, vol. 56, pp. 1859-1864.

B. A. Alsayid, S. Y. Alsadi, J. S. Jallad & M. H. Dradie, "Partial shading of PV system simulation with experimental results", in *Smart Grid and Renewable Energy*, Vol. 4, no. 6, pp. 429-435, 2013.

E. Diaz-Dorado, A. Suarez-Garcia, C. Carrillo & J. Cidnis, "Influence of the shadows in photo voltaic systems with different configuration of bypass diodes", in *International Symposium on Power Electronics Electrical Drives Automation and Motion*, SPEEDAM, pp. 14-16, June 2010.

G. Velasco-Quesada, F. Guinjoan-Gispert, R. Picnic Lopez, Roman-Lumbreras & A. Conesa-Roca, "Electrical PV array Reconfiguration strategy for energy extraction improvement in grid connected systems", *IEEE Trans. Ind. Electron.*, Vol. 56, no. 11, pp. 4319-4331, Nov. 2009.

H. Tian, F. Mancilla-David, K. Ellis, E. Muljadi & P. Jenkins, "Determination of the optimal configuration for a photovoltaic array depending on the shading condition", in *Solar Energy*, vol. 95, pp. 1-12, September 2013.

K. Kurobe & H. Matsunamih, "New two-diode model for detailed analysis of Multicrystalline silicon solar cells", in *Japanese Journal of Applied Physics*, vol. 44, pp. 8314-8321, November 2005.

Mr. Abdulazeez & I. Iskender, "Simulation and experimental study of shading effect on series and parallel connected photovoltaic PV modules", in *Proceedings of the 7th International Conference on Electrical and Electronics Engineering* (ELECO 11), pp. I28-I32, Bursa, Turkey, December 2011.

N. D. Kaushika & A. K. Rai, "An investigation of mismatch losses in solar photovoltaic cell networks", in *Energy*, vol. 32, ISS. 5 pp. 755-759, May 2007.

S. Hamdi, D. Saigaa & M. Drif, "Modeling and Simulation of photovoltaic array with different configurations interconnection under partial shading conditions for fill factor evaluation", in *Proceedings of the International renewable and sustainable Energy Conference* (IRSEC '14), pp. 25-31, IEEE, Ouarzazate, Morocco, October 2014.

V.Quaschning & RHanitsch, "Influence of shading on Electrical Parameters of solar cells", in *Photovoltaic Specialists Conference*, Conference Record of the Twenty Fifth IEEE, pp. 1287-1290, May 1996.

Weidong Xiao, Nathan Ozog & William G. Dunford, "Topology Study of Photovoltaic interface for maximum power point tracking", *IEEE Transactions on Industrial electronics*, Vol. 54, No. 3, June 2007.

Z. Mr Salameh & F. Dagher, "The effect of electrical array reconfiguration on the performance of a PV-powered volumetric water pump", in *IEEE Trans. Energy Convers*, Vol. 5, no. 4, pp. 653-658, December 1990.

Z. Shams El-Dein, M. Kazerani & M. A. Salama,"Optimal Photovoltaic Array Reconfiguration To Reduce partial shading Losses", in *Sustainable Energy IEEE Transactions*, Vol. 4, Issue. I, pp. 145-153, January 2013.